CHAPTER IV

RESULTS AND DISCUSSION

4.1 Preparation of catalysts

In this work, both MgAl and MgGa hydrotalcites were synthesized by alkali-free coprecipitation method utilising $(NH_4)_2CO_3$ and NH_4OH as the precipitation agent [24]. The reason this method was selected was that the conventional preparative routes involving oxide precipitation in the presence of alkali hydroxide and carbonates [25] presented problems of alkali contaminants in the finished catalyst [26]. Its removal was difficult and caused contamination of the product [27, 28].

In hydrotalcites the basic sites in the alkali earth oxides component can originate from O^{2-} (strong basicity), O^- species near hydroxyl groups (medium strength basicity) and OH^- groups (weak basicity). In the synthesis of MgAl hydrotalcite, the addition of Al^{3+} alters the basic properties of the material. Similarly, in the synthesis of MgGa hydrotalcite, replacing Al^{3+} with Ga^{3+} can also modify the basic properties.

4.2 Characterization of catalysts

4.2.1 X-ray diffraction

All synthesized hydrotalcites (MgAl hydrotalcites and MgGa hydrotalcites : as-syn., calcined, and rehydrated) were characterized by XRD technique. The diffractograms are shown in Figures 4.1-4.2 and the results are summarized in Tables 4.1-4.2.
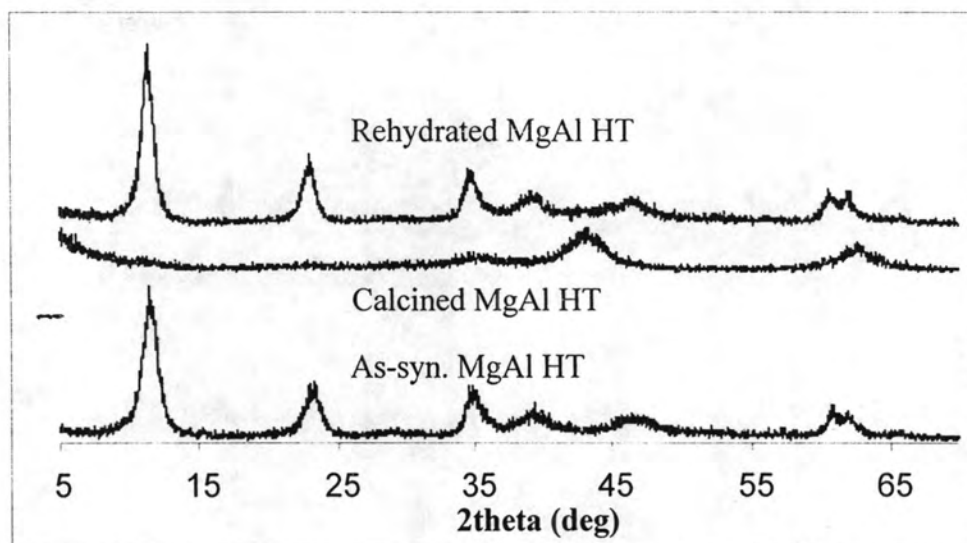
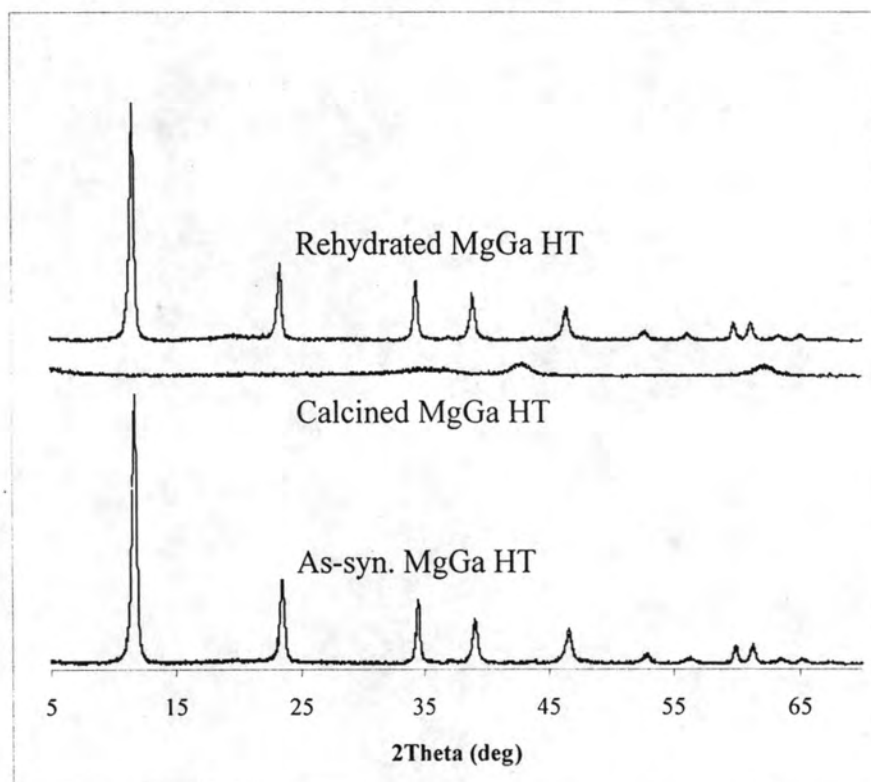**Figure 4.1** Diffractograms of MgAl hydrotalcites.

Figure 4.2 Diffractograms of MgGa hydrotalcites.

Table 4.1 Plane spacings of MgAl hydrotalcites

MgAl Hydrotalcite								
As-syn.			Calcined			Rehydrated		
hkl	2θ(°)	d(Å)	hkl	2θ(°)	d(Å)	hkl	2θ(°)	d(Å)
003	11.6	7.65	111	35.7	2.51	003	11.5	7.69
006	23.4	3.79	200	43.3	2.09	006	23.5	3.79
012	34.8	2.57	220	62.8	1.48	012	34.9	2.57
015	39.0	2.30				015	39.6	2.27
110	60.8	1.52				110	60.8	1.52
113	62.2	1.49				113	62.2	1.49

As shown in the XRD diffractograms (Fig. 4.1), for the as-syn. material, diffraction peaks were observed at 2 angle: 11.6, 23.4, 34.8, 39.0, 60.8 and 62.2 which correspond to the hydrotalcite, the result is in good agreement with that reported [10] 2θ =11.6, 23.4, 35, 39.6, 47.1, 53.4, 56.8, 61.1 and 62.4. The interlayer (d) and unit cell dimensions are shown in Table 4.1 and 4.3, respectively. The unit cell dimensions of as-syn. MgAl hydrotalcite in this work are a = 3.05, c = 2.29 Å, which is in good agreement with that reported [20].

After calcination at 450 °C of the hydrated hydrotalcites, it was found that the diffraction peaks shifted, indicating that the structure of the material was changed. The diffraction peaks were observed at 2θ = 35.7, 43.3 and 62.8 [5] which corresponded to Mg(Al)O phase. The unit cell dimension of cubic system is 4.23 Å.

When performing rehydration on the calcined samples, it was found that the original layered structure can be restored. The diffraction peaks are exactly the same as those of as-syn. hydrotalcite. The result of the rehydration is that the the weak base CO_3^{2-} in the as-syn. hydrotalcite was replaced by the strong Brønsted base OH^-.

In the case of MgGa hydrotalcite, similar behavior as that in MgAl hydrotalcite was found (Table 4.2). When performing calcination, the phase change behavior was also observed. The rehydration of MgGa hydrotalcite can restore the hydrated structure of this hydrotalcite.

Table 4.2 Plane spacings of MgGa hydrotalcites

MgGa Hydrotalcite								
As-syn.			Calcined			Rehydrated		
hkl	$2\theta(°)$	$d(\text{Å})$	hkl	$2\theta(°)$	$d(\text{Å})$	hkl	$2\theta(°)$	$d(\text{Å})$
003	11.7	7.57	111	35.7	2.55	003	11.6	7.64
006	23.4	3.79	200	43.1	2.09	006	23.4	3.80
012	34.5	2.59	220	62.3	1.49	012	34.4	2.60
015	39.1	2.30				015	39.0	2.31
110	59.9	1.54				110	59.9	1.54
113	61.3	1.51				113	61.3	1.51

The lattice parameters of hydrotalcites are shown in Table 4.3. The unit cell parameters a and c were calculated using d_{110} and d_{003} spacing since $a = 2d_{110}$ and $c = 3d_{003}$. The unit cell parameter a shows a dependence on the metal (Mg^{2+}, Al^{3+} and Ga^{3+}). The incorporation of gallium results in slight increase in a parameter a as a consequence of the larger ionic radius of Ga^{3+} cation (0.62 Å) compared to Al^{3+} (0.51 Å). On the other hand, parameter c exhibits no clear-cut trend, as was reported in the literature [29].

Table 4.3 Lattice parameters of hydrotalcites

Unit cell dimensions			
	As-syn. (Å)	Calcined (Å)	Rehydrated (Å)
Material/Crystal system	Hexagonal	Cubic	Hexagonal
MgAl hydrotalcite	a = 3.05, c = 22.90	a = 3.97	a = 3.05, c = 22.90
MgGa hydrotalcite	a = 3.08 , c = 22.72	a = 4.27	a = 3.08, c = 22.89

In this work, apart from the MgAl and MgGa hydrotalcites, MgO oxide has also been synthesized by modified citric acid-ethylene glycol method. The XRD results are shown in Figure 4.3 and plane spacings are summarized in Table 4.4.
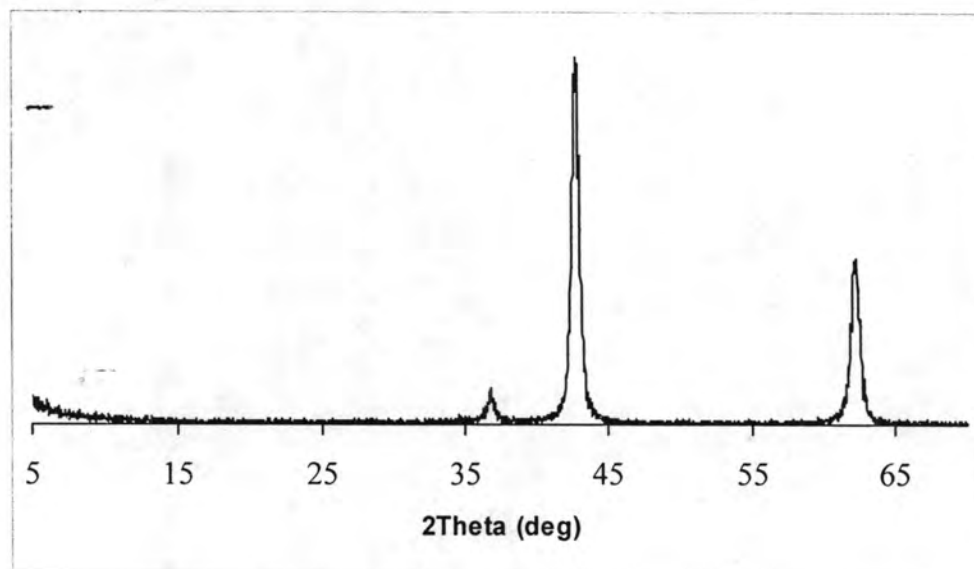

Figure 4.3 Diffractograms of magnesium oxide.

Table 4.4 Plane spacings of magnesium oxide

hkl	$2\theta(°)$	d(Å)
111	36.8	2.44
200	42.8	2.11
220	62.2	1.49

The plane spacings of magnesium oxide determined in this work for MgO is in good agreement with those in the literature [30]. The unit cell dimension is 4.22 Å.

In order to increase the basicity of the catalysts, in this work, some alkali metals and alkali earth metal were loaded onto the calcined hydrotalcites with various %metal. XRD patterns are shown in Figure 4.4.
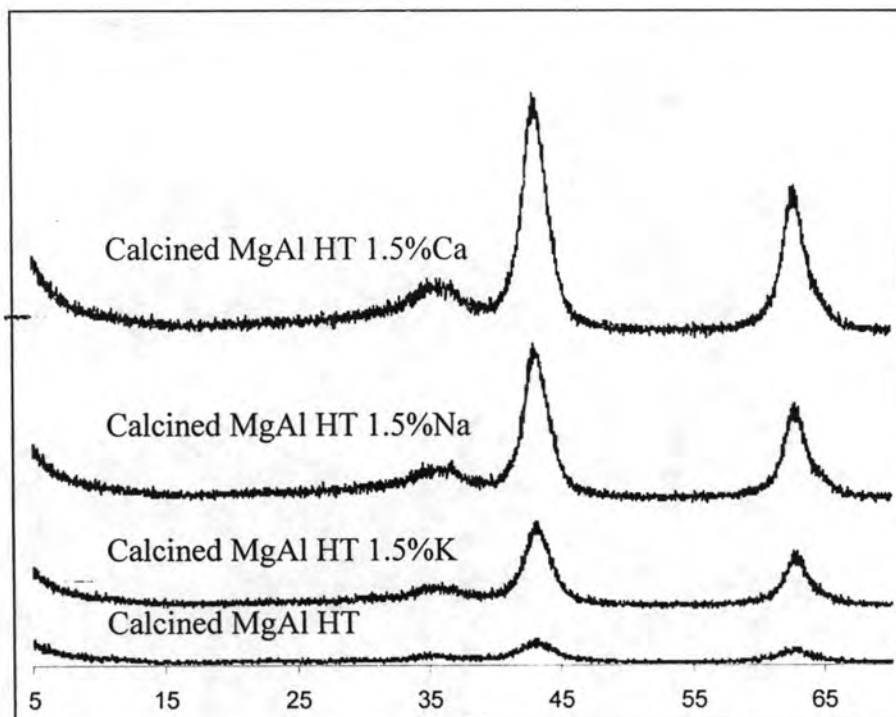
Figure 4.4 Diffractograms of calcined MgAl hydrotalcites loaded with different metal.

In Figure 4.4, the intensity of XRD peaks of the calcined hydrotalcite is low, which reveals low crystallinity. After loading metal, the intensities of diffraction peaks increase intensity. All diffractograms of loaded metal catalysts do not show diffraction peaks of loaded metal, this might be due to very low amount of metal loaded (1.5%).

Table 4.5 Lattice parameters of calcined MgAl hydrotalcites loaded with different metal (1.5%)

K			Na			Ca		
hkl	$2\theta(^\circ)$	$d(\text{Å})$	hkl	$2\theta(^\circ)$	$d(\text{Å})$	hkl	$2\theta(^\circ)$	$d(\text{Å})$
111	35.7	2.51	111	35.7	2.51	111	35.7	2.51
200	43.3	2.09	200	43.3	2.09	200	43.4	2.09
220	62.8	1.48	220	62.8	1.48	220	62.7	1.47

The lattice parameters of calcined MgAl hydrotalcites loaded with different metal (1.5%) was similar to the lattice parameters of calcined MgAl hydrotalcites.

In addition, different % K was loaded onto the calcined MgAl hydrotalcite, the XRD patterns are shown in Figure. 4.5 and summarized in Table 4.6. It can be seen that when amount of K loaded was increased from 0.5% to 1.5%, crystallinity of catalyst was decreased.
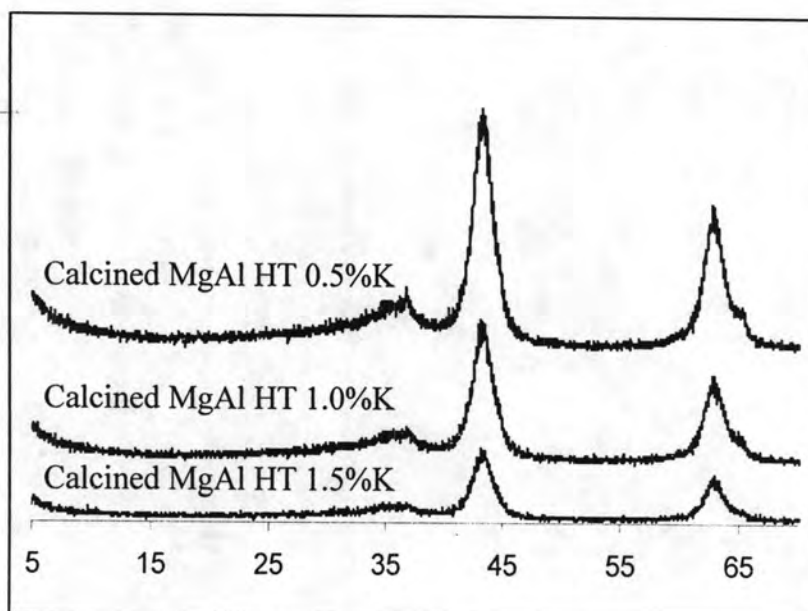

Figure 4.5 Diffractograms of calcined MgAl hydrotalcites loaded with different %K

Table 4.6 Lattice parameters of the calcined MgAl hydrotalcites loaded with different % K

1.5%K			1.0%K			0.5%K		
hkl	2θ(°)	d(Å)	hkl	2θ(°)	d(Å)	hkl	2θ(°)	d(Å)
111	35.7	2.51	111	36.7	4.20	111	36.8	4.22
200	43.3	2.09	200	43.3	4.19	200	43.4	4.17
220	62.8	1.48	220	62.8	4.17	220	62.8	4.17
a = 3.97 Å			a = 3.94 Å			a = 3.94 Å		

4.2.2 SEM analysis

The scanning electron micrographs of the 1.5%K calcined MgAl hydrotalcite and the rehydrated MgAl hydrotalcite were taken as shown in Fig. 4.6.
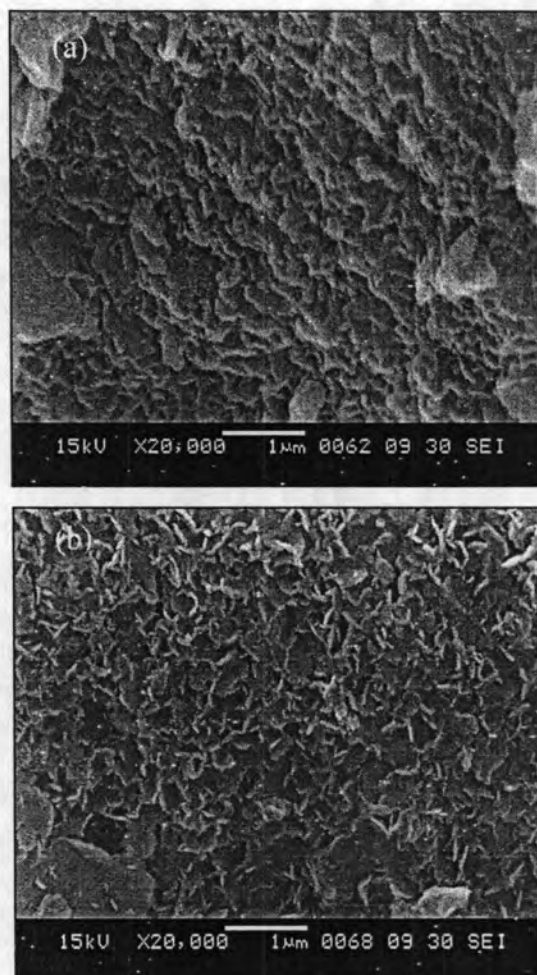

(a)

15kV   X20,000   1μm 0062 09 30 SEI

(b)

15kV   X20,000   1μm 0068 09 30 SEI

Figure 4.6 SEM images of

(a) rehydrated MgAl hydrotalcite (×20,000)

(b) calcined MgAl hydrotalcite loaded with 1.5%K (×20,000)

The SEM photograph of the rehydrated hydrotalcite (Fig.4.6a) revealed layer structure. The SEM photograph of the calcined catalyst loaded with 1.5%K (Fig. 4.6b) showed porosity because the CO_3^{2-} in the interlayer decomposed from the structure.

4.2.3 FTIR (Fourier Transform Infrared Spectroscopy)

All materials were characterized by FTIR, the spectra are shown in Figure 4.7. Peaks assignments are shown in Table 4.7.
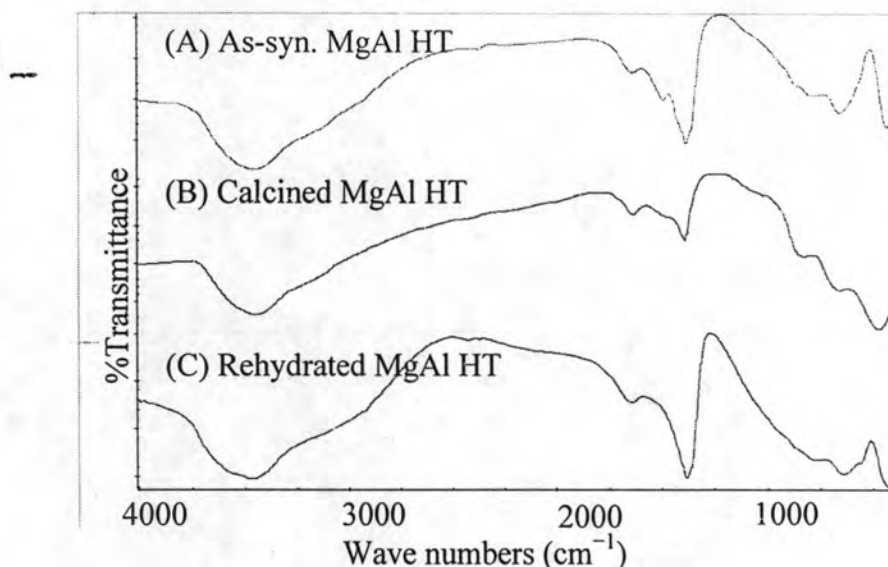

Figure 4.7 FTIR spectra of

(A) As-syn. MgAl HT (B) Calcined MgAl HT and (C) Rehydrated MgAl HT.

Table 4.7 FTIR peak assignments of catalysts

Wavenumber(cm^{-1})			assignment
As-syn. MgAl HT	Calcined MgAl HT	Rehydrated MgAl HT	
3,400-3,500	3,400-3,500	3,400-3,500	vOH stretching
3,050-3,100	3,050-3,100	3,050-3,100	vOH stretching (water)
1,635	1,635	1,635	δOH bending
1,507	-	-	vCO3^{2-} vibrations
1,400	1,400	1,400	vCO3^{2-} vibrations
-	450-650	-	M-O vibrations

The as-syn. hydrotalcite shows IR absorption at about approximately 3400-3500 cm^{-1} which can be ascribed to the vOH stretching vibration of the hydroxyl groups attached to Al and Mg [32]. The shoulder at 3,050-3,100 cm^{-1} suggests the presence of a second type of OH stretching vibration (possibly due to hydrogen bonds of water in the interlayer). It was reported that the intensity of vOH mode decreased with increasing calcination time, indicating the start of layer dehydroxylation. The

minor absorption peak at about 1,635 cm^{-1} could be assigned to δOH bending vibration of H_2O molecule in the interlayer space or absorbed from air [32]. IR absorption at about 1,507 cm^{-1} was attributed to carbonates. The adsorption peak at about 1,400 cm^{-1} typical of O-C-O vibrations in adsorbed (non-interlayer) carbonate on the surface [31]. Thus the bands at 450-650 cm^{-1} correspond to characteristic vibration of the metal oxides [31].

For the calcined MgAl hydrotalcite, after calcination at 450 °C the hydrotalcite structure collapsed to the MgAlO. It was seen that the peak at 1507 cm^{-1} almost disappeared, this means that carbonates in the interlayer were decomposed.

After rehydration, intensity of an absorption at about 1400 cm^{-1} which was attributed to carbonates were high, this might due to the adsorption of carbon dioxide in air atmosphere on the surface of hydrotalcite in the rehydration step[32].

Similar results were obtained for MgGa hydrotalcites, as shown in Figure 4.8 It can be seen that FTIR spectra are similar.
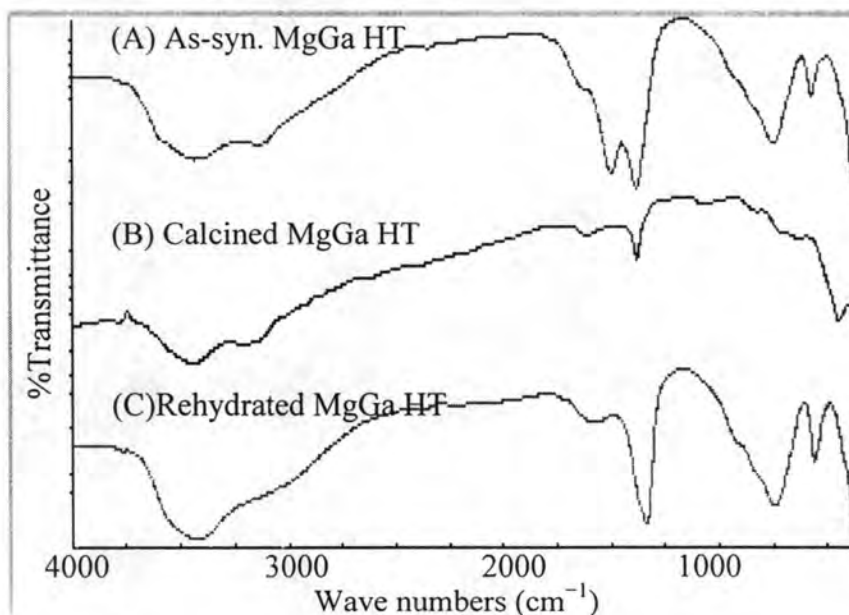

Figure 4.8 FTIR spectra of
(A)MgGa HT (B) Calcined MgGa HT and (C) Rehydrated MgGa HT.

FTIR spectra of calcined MgAl hydrotalcite loaded with different metal are displayed in Figure 4.9.
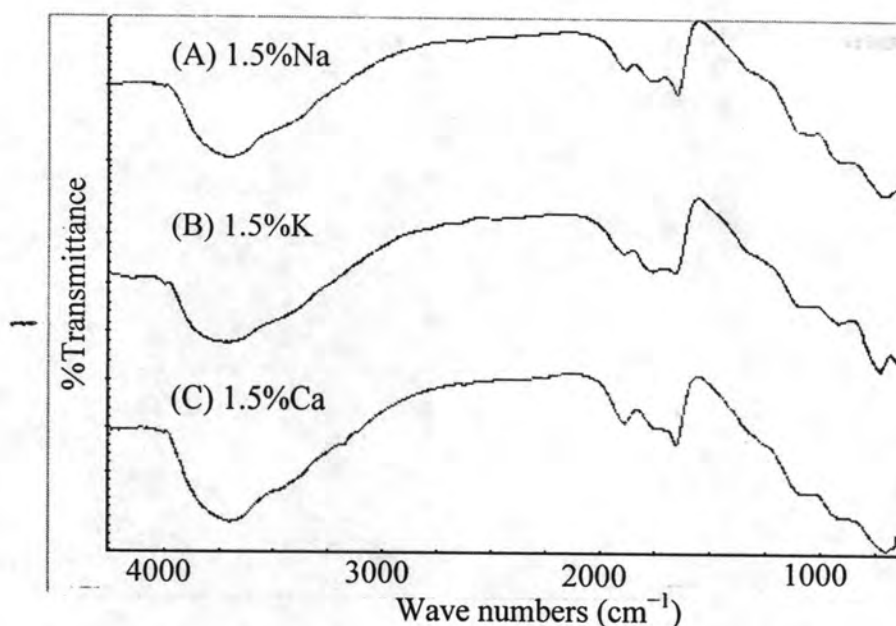
Figure 4.9 FTIR spectra of calcined MgAl hydrotalcite loaded with different metal.

FTIR spectra of the metal loaded-calcined hydrotalcites were similar to that of the calcined hydrotalcite. It should be mentioned that the stretching vibration of Al-O-K group which was reported to appear at around 3500 cm^{-1} [5] cannot be seen in these spectra. This is because of the appearance of water stretching vibration in that region or might be due to very low amount of metal loaded (1.5%).

4.2.4 ICP analysis

The MgAl hydrotalcite was dissolved in nitric acid before analyzed. The ICP analysis showed molarratio of Mg to Al was 2.1. Under the conditions employed there was a deviation between the theoretical (4.0) and observed Mg:Al ratio(2.1), which may be attributed to the low pH used in the preparation. It was reported that higher pHs generally facilitate greater incorporation of Mg into the hydrotalcite [26]. To increase the molar ratio of Mg/Al in the catalyst, another batch of MgAl hydrotalcite was synthesized, using molar ratio of Mg/Al = 5. The ICP analysis showed ratio of Mg to Al was 5.0.

4.2.5 Surface area and porosity of catalyst

BET specific surface areas and porosity of catalysts were tabulated in Table 4.8

Table 4.8 Surface area and porosity of catalysts

| catalyst	% (wt) Metal loaded	BET surface area (m^2/g)	total pore volume (cm^3/g)	mean pore diameter (nm)
calcined MgAl HT	-	243	0.59	9.74
	1.5%Li	129	0.26	8.20
	0.5%Na	152	0.25	6.77
	1.0%Na	143	0.25	6.98
	1.5%Na	135	0.24	7.22
	0.5%K	175	0.30	6.92
	1.0%K	153	0.25	6.45
	1.5%K	140	0.24	6.94
	0.5%Ca	217	0.58	10.84
	1.0%Ca	214	0.56	10.45
	1.5%Ca	207	0.55	10.69
calcined MgGa HT	-	127	0.44	13.97
rehydrated MgAl HT	-	40	0.24	24.57
rehydrated MgGa HT	-	19	0.25	52.89
MgO	-	66	0.34	20.81
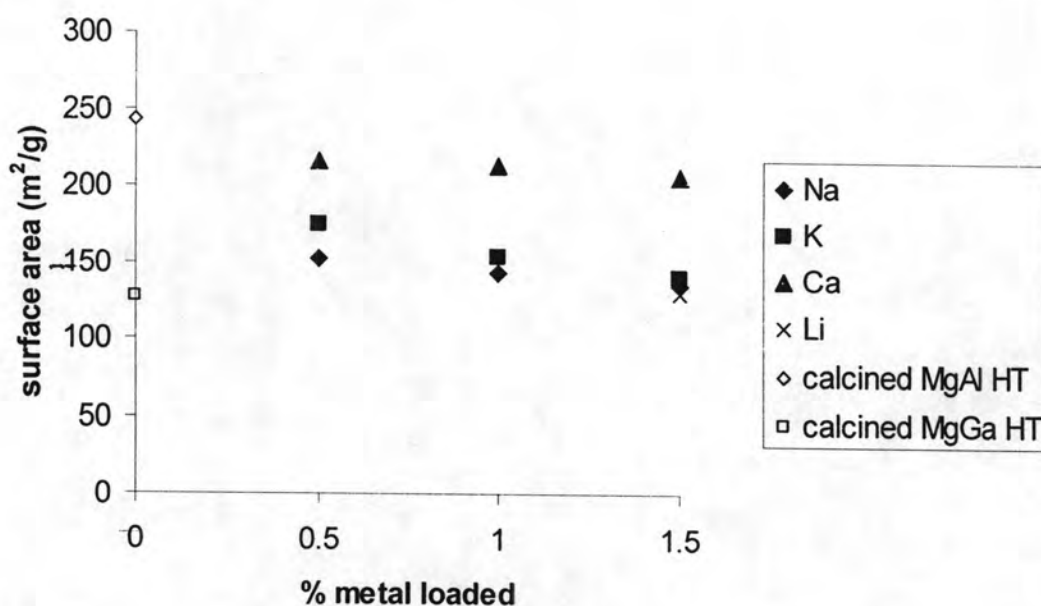
Figure 4.10 Surface area of the calcined hydrotalcite loaded with metal.

The surface areas and porosity of catalysts were determined by BET technique. From the results it was found that the surface area of the calcined hydrotalcites at 450°C was 243 m^2/g, total pore volume was 0.59 cm^3/g and mean pore diameter was 9.74 nm. These values were higher than that previously reported (at the calcinations temperature of 400 °C, surface area of 195 m^2/g, total pore volume 0.43 cm^3/g and mean pore diameter was 9.2 nm were obtained) [34]. The high surface area was resulted from the loss of water and carbon dioxide upon calcination.

When loading metal onto the calcined hydrotalcites, and calcined again at 600 °C, the surface areas and pore volumes were decreased resulting from the incorporation of occluded metal oxide species. The reason to use calcination temperature of 600 °C in this work is because metal acetate was decomposed to metal oxide at around 600 °C.

Considering about the percentage loading of metal, it was found that when % metal loading was increased, the surface area and pore volume were decreased.

Comparing among group I metals, it was found that at the same weight of metal, K loaded catalyst shows higher surface area than Na and Li. In the case of loading group II metal, the surface area and pore volume of the Ca-loaded catalyst changed a little from that of the calcined hydrotalcite.

Comparing between MgAl and MgGa hydrotalcites, (both calcined and rehydrated) it can be seen that the MgAl hydrotalcite has higher surface area than MgGa hydrotalcite.

As the calcination temperature is one factor which can affect the characteristic of the material, therefore, in this work, calcination temperature was changed to higher temperature, 600°C. The surface area was found to be 190 m^2/g, total pore volume 0.73 cm^3/g and mean pore diameter is 15.32 nm. These are different from those calcined at 450°C. The surface area of the catalyst calcined at 450°C is higher. Therefore 450°C was used for all experiments.

MgO which was synthesized in this work has the surface area of 66 m^2/g which is lower than that of hydrotalcite.

4.2.6 Basicity

To determine the basicity of the catalysts, the catalysts were stirred in distilled water for 1 h before filtration. Then the filtrate was titrated with 0.02 M benzoic acid solution (in methanol). The soluble basicity of the catalysts are shown in Table 4.9.

Table 4.9 Basicity of catalysts

Catalyst	Condition	%metal loaded	Basicity (mmol/g)
MgAl HT	Rehydrated	-	0.02
	Calcined	-	0.05
	Calcined	1.5%Na	0.43
	Calcined	1.5%K	0.27
	Calcined	1.5%Ca	0.14
	Calcined	1.0%K	0.13
	Calcined	0.5%K	0.06
MgGa HT	Rehydrated	-	0.03
	Calcined	-	0.04
MgO	-	-	0.10

For the rehydrated MgAl and MgGa hydrotalcites, they have comparable basicity (0.02-0.03)

Also, the basicity of the calcined MgAl and MgGa hydrotalcites are comparable (0.04-0.05). However, the basicity is lower than that of MgO. Al is more electronegative than Mg, an increase in Al should increase the average electronegativity of the catalyst, and thus, a decrease in the average electronic density of the unsaturated framework oxygens could be expected, with the corresponding effect on their basicity and catalytic activity [32, 34, 35]. Therefore, the basicity of coordination of Mg^{2+} with O^{2-} is higher than that of Al^{3+} with O^{2-} [36].

The basicity for the calcined HT loaded with 1.5%Na and 1.5%K were 0.43 and 0.27 mmol/g, respectively. The higher basicity of the Na loaded catalyst can be accounted from the amount of metal as the atomic weights of Na and K are different. The atomic ratios of Na: K are 1.5:1 [35]. It was also seen that the basicty of loaded metal catalysts was increased when the percent of metal loaded increased. The basic sites in the alkali earth oxides component can originate from O^{2-} (strong basicity), O^- species near hydroxyl groups (medium strength basicity) and OH^- groups (weak basicity).

4.3 Transesterification of tributyrin

4.3.1 Type of hydrotalcite

The catalytic transesterfications of tributyrin (as a model compound) with methanol using a series of hydrotalcites catalysts were investigated for the same period of time under the same condition.

Representative chromatograms from the transesterification of tributyrin were shown in Figure 4.11. It was seen that tributyrin was transesterified with methanol to yield methyl butanoate as reaction product, together with some amount of dibutyrin and monobutyrin.

It should be mentioned that these conditions were not optimized to obtain highest reaction yield; however, they provided a comparative study of the catalysts' activity. The activity was reported as %conversion of tributyrin. The data of %conversion and peak area ratios of tributyrin, dibutyrin and monobutyrin were also tabulated in Table 4.10.
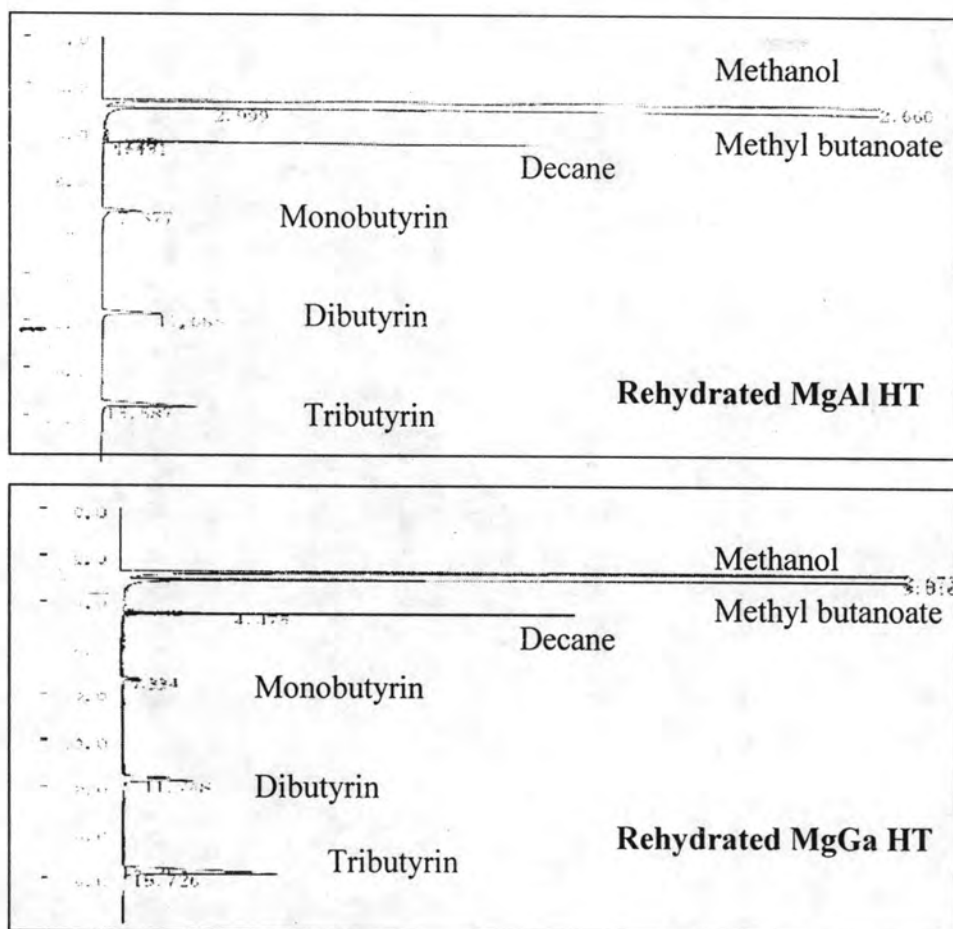
Figure 4.11 GC chromatograms of transesterification of tributyrin using rehydrated MgAlHT (above) and rehydrated MgGaHT.(below)

Table 4.10 Transesterification of tributyrin

Entry	Catalyst	Tributyrin conversion (%)	peak area ratios TB: DB: MB
1	MgAlHT, calcined	32.7	1: 0.2: 0
2	MgAlHT, rehydrated	76.4	1: 0.6: 0.4
3	MgGaHT, calcined	14.3	1: 0.1: 0
4	MgGaHT, rehydrated	49.8	1: 0.3: 0.1

Reaction condition: 0.05 g catalyst (1.5wt%), 0.01 mol (3 ml) tributyrin, 0.30 mol (12.5 ml) methanol, methanol/tributyrin molar ratio = 30 , temperature 60 °C, time 3 h. TB(tributyrin), DB(dibutyrin), MB(monobutyrin)

Comparison of the calcined and rehydrated hydrotalcites showed that the rehydrated HT shows much higher conversion (76.4%) than the calcined HT (32.7%). This is in good agreement with that reported previously (74.8%) [20]. This can be explained by the higher basic strength of hydroxyl group compared to the lone pair of electron on oxygen. The rehydrated MgAl HT shows much higher conversion than MgGa HT. This might be due to the higher surface area of MgAl HT (see Table 4.8). Another reason is that Ga is more electronegative than Al, the Ga incorporation decreases the electron density of the framework oxygens.

Furthermore, when considering ratios of tributyrin, dibutyrin and monobutyrin, it can be seen that the better catalyst gave a more complete transesterification reaction as can be seen from the higher amounts of monobutyrin and dibutyrin. In the rehydrated MgAl HT catalyst, the peak area ratios of tributyrin:dibutyrin: monobutyrin = 1: 0.6: 0.4 which means that tributyrin can be converted more completely than that of the rehydrated MgGa HT catalyst. Therefore, the MgAl HT was selected for further experiments.

4.3.2 Metal-loaded hydrotalcite

In addition, in this work, group I and II metals were also loaded in various amounts (0.5, 1.0, 1.5 wt%) onto the synthesized hydrotalcite by incipient wetness impregnation. The metal-loaded catalyst was used for transesterification of tributyrin. The results are shown in Table 4.11.

Table 4.11 Transesterification of tributyrin using metal-loaded catalysts

Entry	Calcined MgAl HT loaded with metal (wt%)	Tributyrin conversion (%)
1	0	32.7
2	0.5%Na	36.9
3	1.0%Na	48.4
4	1.5%Na	68.4
5	0.5%K	39.6
6	1.0%K	54.7
7	1.5%K	77.8
8	1.5%Ca	7.8
9	1.0%Ca	13.1
10	0.5%Ca	17.3
11	1.5%Li	5.7

Reaction condition: 0.05 g catalyst (1.5wt% based on tributyrin), 3 ml tributyrin, 12.5 ml methanol, molar ratio of methanol to tributyrin = 30, temperature 60 °C, time 3 h.

The catalytic activities of the metal-loaded catalysts were compared at the same condition, 0.05 g catalyst, 0.01 mol (3 ml) tributyrin, 0.3036 mol (12.5 ml) methanol at temperature 60 °C, time 3 h. The activities of the calcined hydrotalcites loaded with metal were higher than the one without metal loading. The results showed that the catalytic activities increased with the amount of metal loading. This might be result from an increasing number of basic sites on hydrotalcites. Activity order of the metal is corresponded to the basic strength of the metal as follows: K > Na > Li, following the order of electropositivity of the metal [7]. In the case of Ca-loaded catalyst, it showed lower %conversion of tributyrin.

4.3.3 Type of potassium salts

As can be seen from the above results that potassium is the best among many metals tested. Therefore, several kinds of potassium salts loaded onto the calcined hydrotalcite were compared. The result are shown in Figure 4.12.
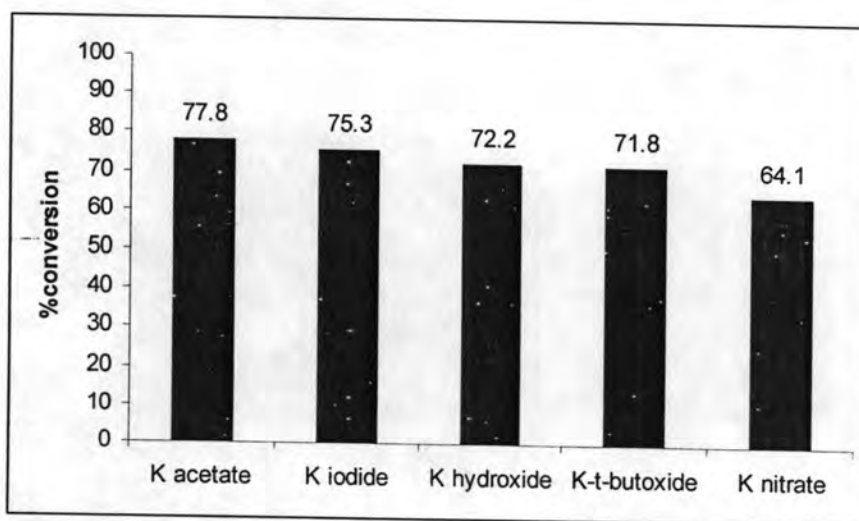

Figure 4.12 Conversion of tributyrin using hydrotalcites loaded with different K salts (1.5%loading).

The results showed that among the K salts tested in this work, potassium acetate was found to display slightly higher conversion than others. K nitrate seems to have lowest activity. However, activities are not much different. It was reported that in the transesterification of soybean oil with methanol using potassium supported alumina, the conversion to methyl esters over the catalysts is in the following order: $KOH > KNO_3$ [33]. This order is opposite to the order of their thermal stability in air, which probably suggests that their different catalytic activities should be attributed to their different decomposition extents in air, and therefore, the K_2O species derived from the decomposition process possibly being the main catalytically active species [33].

In addition, different sodium salt with the same wt% (1.5%) was also investigated in this work. It was found that using sodium acetate (68.4% tributyrin

conversion) was a better salt than sodium azide (NaN$_3$) (54.5%). This result was in contrast to that previously reported [7].

4.3.4 Magnesium oxide

For comparison, MgO which was widely studied for transesterification of vegetable oil, was also studied in this work compared the calcined hydrotalcite catalyst. The catalytic activity of MgO was 35% tributyrin conversion. The result was similar to the calcined MgAl hydrotalcite catalyst (32.7% tributyrin conversion).

4.3.5 Test of metal leaching from catalysts

In this work, test of leaching of metal from the catalyst was also investigated, because leaching was the main problem which usually occur for the metal–loaded catalyst. The catalyst (0.05 g) was stirred in 12.5 ml methanol at 60 °C for 1 h and then was filtered by a filter paper. The filtrate was used for transesterification of tributyrin to observe any leaching of metal from the catalyst. The result showed that when loading high amount of metal (4 wt% metal), about 70-84% tributyrin conversion was obtained and the 1.5 wt% potassium showed 10% tributyrin conversion. This clearly revealed that metal was leached from the catalyst. However, for MgO slight leaching was detected.

4.4 Hydrotalcite exchanged with tert-butoxide

The rehydrated hydrotalcite was anion exchanged with tert-butoxide. XRD diffractogram of the exchanged hydrotalcite is shown in Fig. 4.13. Its diffractogram is the same as the rehydrated hydrotalcite.

The IR spectrum is shown in Fig.4.14. The stretching signal of C-H bond at 2973 cm^{-1} from tert-butoxide was not obtained [37]. This reveals that no exchange occurred between tert-butoxide and the OH⁻ anion interlayer. The preparation in this work is different from that was reported in the literature [16] in which MgAl tert-butoxide was synthesized by anion nitrate and then ion exchanged with the tert-

butoxide ion. But in this work, the hydrotalcite was prepared from metal carbonate, then the carbonate was replaced with hydroxide, followed by tert-butoxide exchange. It was reported that the affinity of hydrotalcite for interlayer anions is the following order: $CO_3^{2-} \gg SO_4^{2-} \gg OH^- > F^- > Cl^- > Br^- > NO_3^-$ [38]. The NO_3^- interlayer can be exchanged by the tert-butoxide more easily than the OH^- interlayer. Therefore, we conclude that in this work the exchanged hydrotalcite was not obtained. Moreover, the low activity (6.5% tributyrin conversion) could be due to water adsorbed on the catalyst. It was reported that the excess of water can cause catalyst decay or active site inhibition [19].
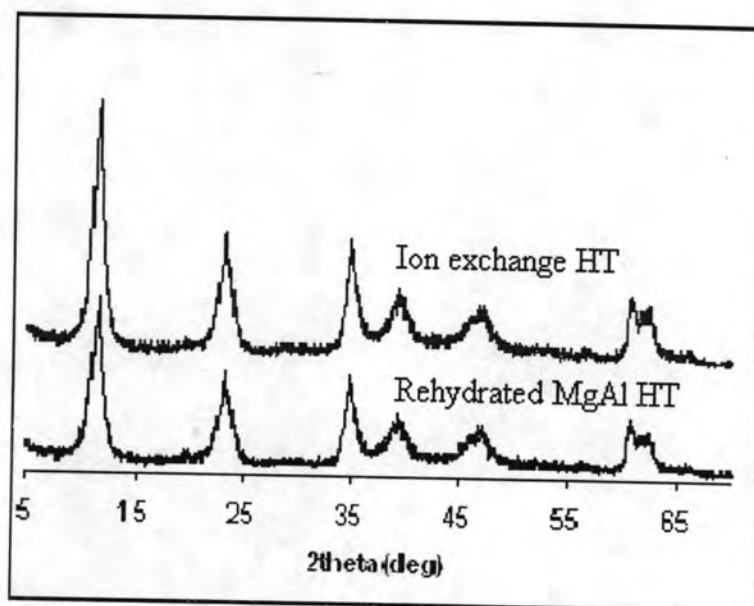
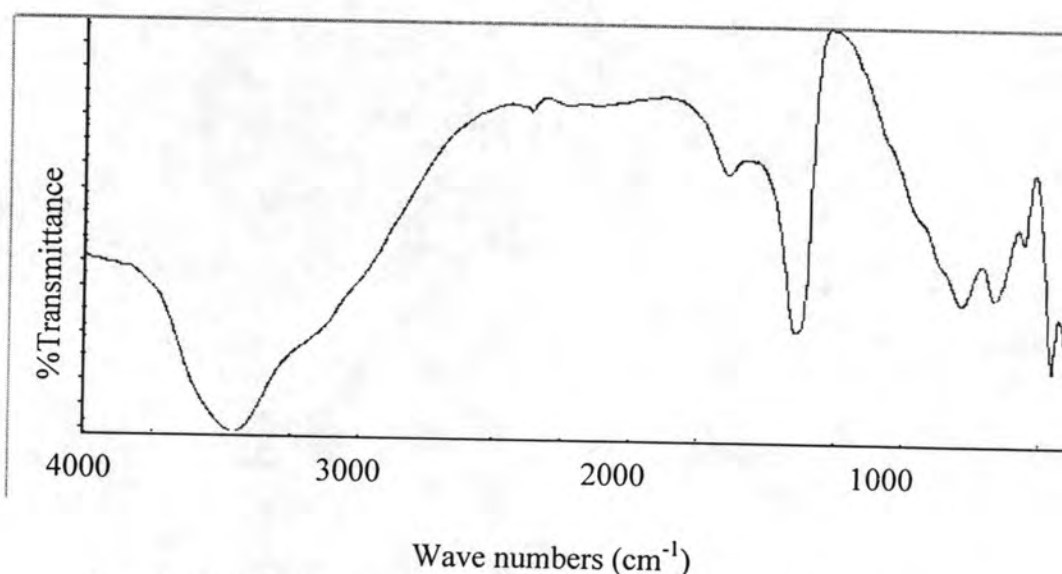Figure 4.13 XRD diffractograms of hydrotalcite exchanged with tert-butoxide.

Wave numbers (cm^{-1})

Figure 4.14 FTIR spectrum of hydrotalcite exchanged with tert-butoxide.

4.5 Transesterification of refined palm oil

Composition of refined palm oil was determined by Ce 2-66, Ce 1-62 AOCS 1993. The results are shown in Table 4.12.

Table 4.12 Composition of refined palm oil

Fatty acid	(%)
C16:0 Palmitic acid	42.3
C18:0 Stearic acid	3.3
C18:1 Oleic acid	44.5
C18:2 Linoleic acid	9.9

It was found that the palm oil mainly consisted of unsaturated fatty acid, oleic acid and palmitic acid. FFA, free fatty acid of refined palm oil was determined following the standard method, it was 0.36 mg KOH (acid value).

4.5.1 Effect of reaction time

Refined palm oil was used to produce biodiesel using 1.5%K-loaded HT catalyst. The product yield and ester content were monitored with time at 12, 15, 18 h. The results are displayed in Figure 4.15. The ester content and product yield increased with reaction time and was nearly 90% ester content after 15 h. Fig. 4.16 shows a respresentative GC chromatogram.
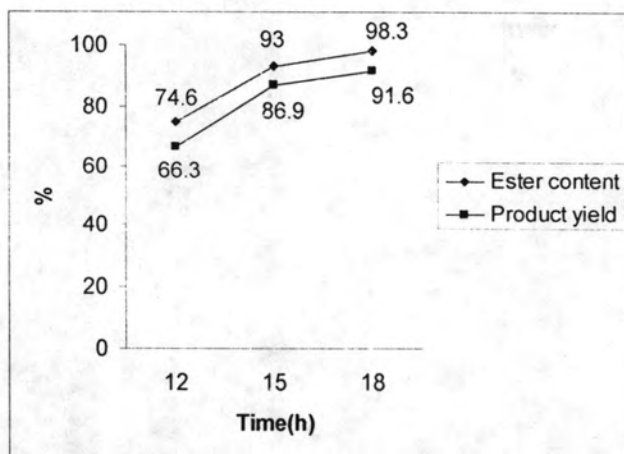
Figure 4.15 Ester content and product yield vs time.
Reaction conditions: 1.5 % K-loaded MgAl HT catalyst 7.5wt%, MeOH/oil molar ratio 45:1, temperature 60°C


```
C-88A CHROMATOPAC CH=1   Report No.-2      DATA 1:8CHRM1.C00   07 03 20  15:43 26

** CALCULATION REPORT **
CH PKNO   TIME      AREA      HEIGHT    MK   IDNO   CONC       NAME
1    1    2.038    1632361    1000851   E           92.4633
     2    8.285      15324       3148               0.868
     4   21.031      44780       3612               2.5365
     5   26.021      11317       1042               0.641
     6   26.483      56549       3946    V          3.2031
     7   27.215       5086        652    V          0.2881

         TOTAL     1765415    1013250             100
```
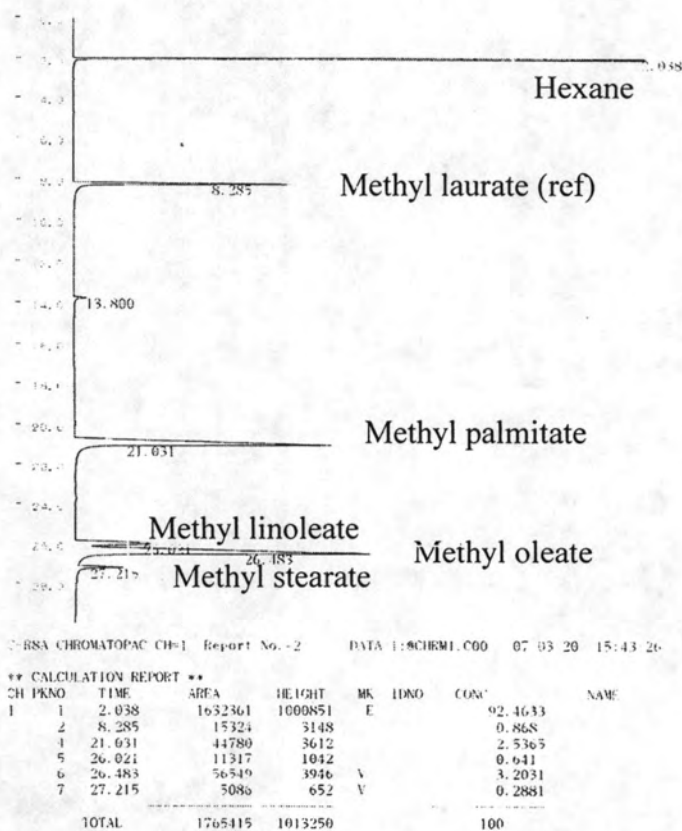
Figure 4.16 GC chromatogram from transesterification of refined palm oil using 1.5%K-loaded MgAl HT at 18 h.

A respresentative GC chromatogram from transesterification of refined palm oil shows esters products (methyl oleate and methyl palmitate were main products) with the following elution times:

methyl laurate (reference) at 8.32 min

methyl palmitate at 21.12 min

methyl linoleate at 26.06 min

methyl oleate at 26.60 min

methyl stearate at 27.28 min.

4.5.2 Effect of catalyst amount

Effect of catalyst amount was investigated. The results are shown in Table 4.13.

Table 4.13 Transesterification of refined palm oil at different amounts of catalyst

wt% catalyst	methanol/oil molar ratio	Product yield (%)	Ester content (%)
7.5%	45:1	84.3	90.5
5.0%	45:1	72.7	81.0

Reaction conditions: 1.5 % K-loaded MgAl HT catalyst, temperature 60°C, time 18 h

From Table, it can be seen that when the amount of catalyst was decreased from 7.5 to 5.0% the ester content and product yield were also decreased.

4.5.3 Effect of reaction temperature and pressure

To increase rate of reaction, higher reaction temperature was used (100 and 120 °C). The reactions were performed in a Parr reactor which can withstand high pressure created under high temperature. The pressure was read with pressure gauge of the Parr reactor. Experiment in the absence of catalyst was also performed. The results are shown in table 4.14.

Table 4.14 Transesterification of refined palm oil using 1.5wt%K

Entry	Pressure (atm)	temperature (°C)	time (h)	Product yield (%)	Ester content (%)
1*	3	100	9	0.4	0.6
2	3	100	9	85.6	93.7
3	5	120	9	58.9	69.0

Reaction conditions: 1.5 % K-loaded MgAl HT catalyst 7.5wt%, MeOH/oil molar ratio 45:1

* absence of catalyst

In entry 1, in the absence of the catalyst, product yield and ester content are very low (0.4% and 0.6%, respectively). In entry 2, the product yield and ester content at temperature of 100°C are 85.6% and 93.7%, respectively which are higher than those at 60°C (Table 4.13). It should be mentioned that in this work, the reactions at high temperature were performed in a Parr reactor, pressure inside the reactor increased with increasing temperature. Therefore, the higher conversion obtained when increasing temperature resulted from the pressure created (which was measured to be 3 atm), this result is similar to that reported [38].

However, when the temperature was increased to 120°C (entry 3), the ester content and product yield were decreased (58.9% and 69.0%, respectively). This might be due to the formation of soap from the saponification of glycerides by the alkaline catalyst before completion of the alcoholysis [39] which was accelerated at high temperature.

4.5.4 Effect of molar ratio of methanol/oil

The molar ratio of methanol to palm oil is one of the important factors that affect the conversion to methyl esters. Stoichiometrically, three moles of methanol are required for each mole of triglyceride, but in practice a higher molar ratio is employed in order to drive the reaction towards completion and produce more methyl esters as products.

Table 4.15 shows the effect of methanol/oil molar ratio on %ester content and %product yield.

Table 4.15 Transesterification of refined palm oil

Mg/Al nominal	molar ratio methanol/oil	Pressure (atm)	temperature (°C)	time (h)	Product yield (%)	Ester content (%)
4	45	3	100	9	85.6	93.7
4	30	3	100	9	54.1	79.9

Reaction conditions: 1.5 % K-loaded MgAl HT catalyst 7.5wt%

When the methanol amount was decreased (molar ratio of methanol/oil = 30), it was found that ester content and product yield were decreased considerably. The soap formation was observed, affecting the product yield. High amount of methanol was needed for a good product yield.

4.5.5 Effect of %potassium loading

Table 4.16 Transesterification of refined palm oil using different %K loaded

%K	Pressure (atm)	temperature (°C)	time (h)	Product yield (%)	Ester content (%)
1.5%K	3	100	9	85.6	93.7
4.0%K	3	100	9	73.2	91.3

Reaction conditions: K-loaded MgAl HT catalyst 7.5wt%, MeOH/oil molar ratio 45:1

From the results, it was seen that the higher %K loading did not improve product yield and ester content. On the contrary, it was seen that product yield was decreased significantly. Moreover, it caused a problem of metal leaching from the catalyst. When testing leaching, it was found that the filtrate from 4.0%K catalyst showed 55.8% ester content. In the experimental, it was observed that soap formation

is high. The metal leaching from the catalyst cause undesirable saponification reaction which reduces the product yield and considerably disturbs the recovery of the glycerol due to the formation of emulsions [4].

4.6 Reusability of the catalysts

In order to study the stability of the catalyst, after experiment in Table 4.15, the 1.5%K-loaded MgAl HT catalyst was reused by being filtered, washed thoroughly with methanol and heated in an oven at 100 °C for 12 h before being used again. The results are shown in Table 4.17.

Table 4.17 Reusability of the catalyst

| use	Ester content (%)
first use	90.5
reused	20.4
reloaded K	81.4

Reaction conditions: 1.5%K-loaded MgAl HT catalyst, 7.5wt%, MeOH/oil molar ratio 45:1, temperature 60°C, time 18 h

After first use, a decline in activity was observed, the ester content decreased from 90.5% to 20.4%. Such a decrease in the catalytic activity was, probably, responsible for leaching of the K_2O species from the supported catalyst. In addition, the glycerol which might be adsorbed on the catalyst inactivate the active site on the surface catalyst. This can be confirmed by analyzing the amount of remaining K in the catalyst.

The used catalyst was regenerated by impregnating 1.5 wt% K again (as described in the experimental section). The results showed that the reloaded K catalyst give ester content of 81.4%, thus suggesting that the catalyst could be regenerated by this method.

4.6 Proposed mechanism

The mechanism of the base-catalyzed methanolysis of esters for tributyrin using rehydrated MgAl HT catalyst and palm oil using 1.5%K-loaded MgAl HT catalyst are proposed in Schemes 1 and 2.
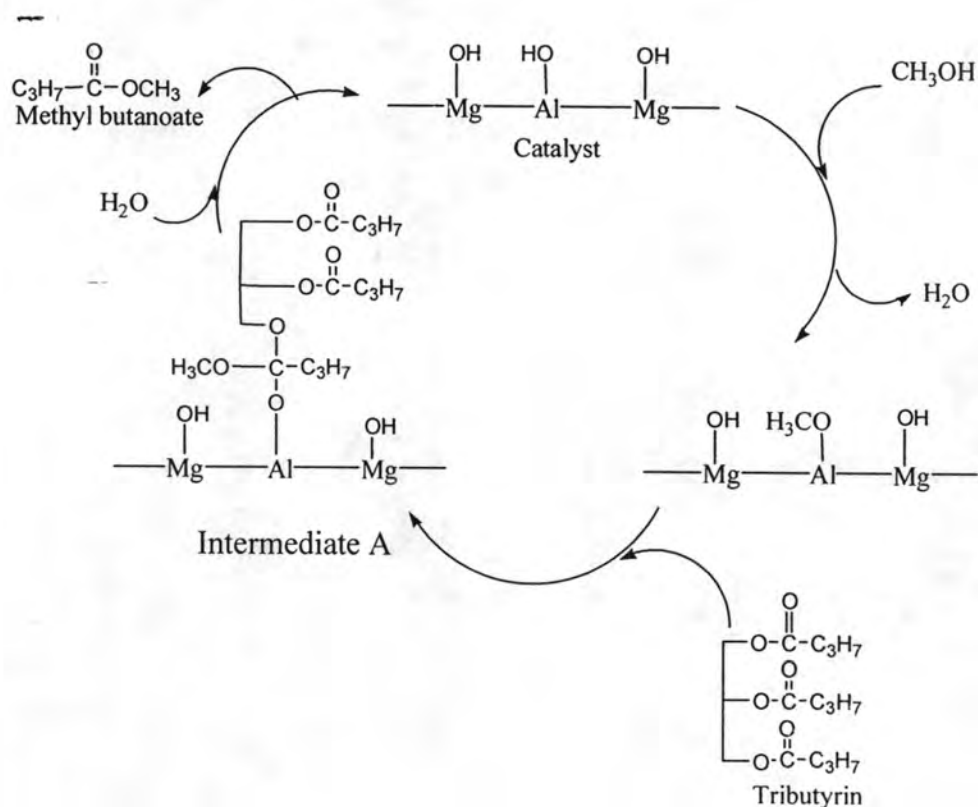
Scheme 1. Mechanism of transesterification of tributyrin using rehydrated hydrotalcite catalyst.

The rehydrated hydrotalcite lattice comprises layered structure of positively charged bimetallic layers compensating with OH- anions in the interlayer. In the first step, the abstraction of proton from methanol results in the formation of methoxide anion, stabilised by the cationic charge of the aluminium in the lattice of the hydrotalcite. Then, in the next step, the formed methoxide can be further stabilised with carbonyl ester of oxygen due to high electronegativity of oxygen atom present on carbonyl ester to form an intermediate A. This intermediate reacts with H_2O to yield final transesterified product, methyl butanoate.
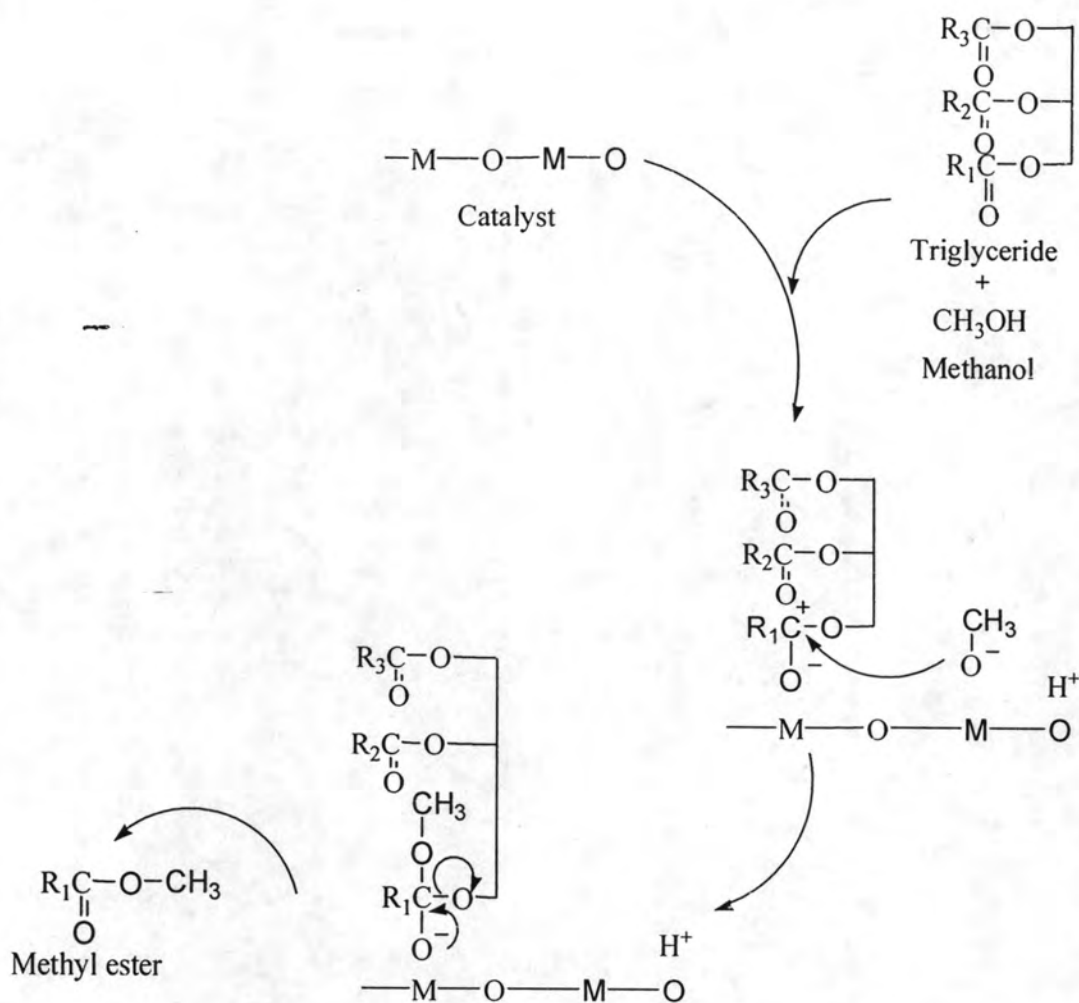
Scheme 2. Mechanism of transesterification of palm oil using metal-loaded calcined hydrotalcite catalyst.

The transesterification process of palm oil consists of a sequence of three consecutive reversible reactions where the triglyceride is successively transformed into diglyceride, monoglyceride, and finally into glycerin and the fatty acid methyl esters.

The proposed reaction mechanism shown in Scheme 2 is similar to that for the tributyrin in Scheme 1. The first step describes the adsorption of methanol and triglyceride on two neighboring free catalytic sites of the metal-loaded calcined hydrotalcite catalyst. The two adsorbed species then react to form a surface intermediate that further converted to methyl ester [18].

Table 4.18 Comparison of the result from this work with other works

Catalyst	Condition	Product yield (%)	Ester content (%)	Conversion	Reference
1.5%K calcined hydrotalcite	T = 100 °C t = 9 h wt% cat = 7.5% methanol/palm oil molar ratio = 45	85.6	93.7	-	This work
calcined hydrotalcite	T = 60 °C t = 20 h wt% cat = 7.5% methanol/soybean oil molar ratio = 15	-	-	65	[5]
35 wt.% KNO_3 loaded- Al_2O_3	T = 60 °C t = 7 h wt% cat = 6.5% methanol/soybean oil molar ratio = 15	-	-	87	[40]
ETS-10	T = 150 °C t = 24 h wt% cat = 1.5% methanol/soybean oil molar ratio = 6	-	95.8	-	[7]